Vol. 644: 15–31, 2020
https://doi.org/10.3354/meps13361

MARINE ECOLOGY PROGRESS SERIES
Mar Ecol Prog Ser

Published June 25

Effects of different plankton communities and spring bloom phases on seston C:N:P:Si:chl *a* ratios in the Baltic Sea

Tobias Lipsewers[1,2,*], Riina Klais[3], Maria Teresa Camarena-Gómez[1,4], Kristian Spilling[1]

[1]Finnish Environment Institute (SYKE, Marine Research Centre), 00790 Helsinki, Finland
[2]Faculty of Biological and Environmental Sciences, University of Helsinki, 00014 Helsinki, Finland
[3]Ecostat Ltd, 50605 Tartu, Estonia
[4]Tvärminne Zoological Station, University of Helsinki, 10900 Hanko, Finland

ABSTRACT: Plankton communities and their temporal development have shifted towards earlier onset of the spring bloom and lower diatom–dinoflagellate proportions in parts of the Baltic Sea. We studied the effects of community composition and spring bloom phases on seston nutrient stoichiometry, revealing possible consequences of these shifts. Community composition, seston C:N:P:Si:chl *a* ratios, and physiological and environmental variables were determined for 4 research cruises, covering all major sub-basins and bloom phases. A redundancy analysis revealed that temperature and inorganic nutrients were the main drivers of community changes, and high diatom biomass was linked to low temperatures (growth phase). The effects of changing dominance patterns on seston stoichiometry were studied by applying a community ordination (non-metric multidimensional scaling and generalized additive models). C:N:P ratios increased from the growth phase (103:14:1) to the peak phase (144:18:1) and decreased after inorganic nitrogen was depleted (127:17:1). Taxonomic differences explained ~50% of changes in C:Si, N:Si, and chl *a*:C ratios and <30% for C:P and N:P, whereas C:N was virtually unaffected by the community composition. The fixed chl *a*:C range (~0.005–0.04) was largely determined by diatoms, independent of the dominant species. Thus, C:Si and N:Si could be used to estimate the share of diatoms to the seston and chl *a*:C to describe bloom phases and C budgets during spring. Interestingly, mixed communities featured higher C:N:P ratios than diatom-dominated ones. However, as community composition explained <30% of changes in C:N:P, we conclude that these ratios rather represent the total plankton physiology in natural plankton assemblages.

KEY WORDS: Plankton stoichiometry · Diatoms · Dinoflagellates · Heterotrophs · Natural communities · Particulate organic nutrients

1. INTRODUCTION

The seston comprises all particles suspended in natural waters, and is largely dominated by phytoplankton (major autotrophs in aquatic systems) during bloom events. Additionally, the seston plays a major role in the flux of energy and elements in marine ecosystems (Frigstad et al. 2011). The phytoplankton community forms the base of the food web and is responsible for 40 to 60% of the annual global photosynthesis (Falkowski & Raven 1997). By fixing inorganic C and taking up dissolved inorganic nutrients from surface waters, phytoplankton affects the concentrations of key elements such as C, N, P, and

*Corresponding author: tobias.lipsewers@gmail.com

Si and plays an essential role in global biogeochemical cycles (Field et al. 1998, Harris 1999, Arrigo 2005).

Based on findings by Redfield (1934) and Fleming (1940), the average atomic ratio of C:N:P in marine plankton of 106:16:1 is usually called the Redfield ratio (Redfield 1958). This ratio is frequently used as an indicator to identify limiting nutrients and estimate the limitation intensity (Hecky & Kilham 1988, Tyrrell 1999, Sterner & Elser 2002). However, the phytoplankton C:N:P ratio may diverge substantially from the Redfield ratio due to changes in environmental conditions (e.g. inorganic nutrient concentrations, temperature, and light), different growth phases, variations in taxonomic composition, and changes in microbial metabolism such as N fixation (Klausmeier et al. 2004, 2008, Finkel et al. 2006). Different cellular components have characteristic elemental compositions, and their concentrations in the cell vary between different growth phases: proteins and chl *a* do contain N but little or no P, whereas rRNA is rich in both N and P. Additionally, cellular stoichiometry is regulated by nutrient storage processes, the activity of enzymes, and modifications of the cellular osmolyte composition (Sterner & Elser 2002, Klausmeier et al. 2004). Variations in the C:N:P:Si:chl *a* stoichiometry may affect zooplankton growth, food web dynamics, and the remineralization of nutrients. Although the variability in stoichiometry has been studied thoroughly in cultures (reviewed in Moreno & Martiny 2018), an understanding of the underlying mechanisms from seasonal to long-term time scales across different ocean regions is still missing (but see, e.g., Talarmin et al. 2016). This is unfortunate, as the balance between C, N, and P is important for major biogeochemical pathways. Even minor changes in organismal uptake of these nutrients may have large implications for global biogeochemical cycles (Ducklow et al. 2001). Projected changes in temperature, CO_2, and O_2 concentrations in the sea will likely alter the patterns of dominating plankton groups with consequences for ecosystem structure and biogeochemistry (Boyd et al. 2015). These shifts in phytoplankton dominance patterns may affect biogeochemical cycling as the C:N:P stoichiometry and export potential (C and nutrients) of different communities vary (Spilling et al. 2018).

The Baltic Sea is one of the world's largest brackish water systems. During the spring bloom, ~50% of the annual C fixation occurs in only ~1 mo (Lignell et al. 1993, Heiskanen 1998). Limited water exchange with the North Sea and the environmental pressures caused by ~85 million people inhabiting the Baltic Sea catchment area have led to severe problems, most notably eutrophication. Excessive concentrations of inorganic nutrients have caused increased phytoplankton biomass, and thus water turbidity, and spreading of O_2-depleted bottom waters (HELCOM 2018). Temperature is known to be an important driver of phytoplankton community composition, and the spring bloom species in the Baltic Sea are cold water adapted (Niemi 1973, Okolodkov 1999). A warming climate has caused an earlier onset of the spring bloom (Groetsch et al. 2016) and an extended growing season (Wasmund et al. 2019), and phytoplankton community composition has shifted to higher dinoflagellate proportions at the expense of diatoms (Wasmund & Uhlig 2003, Klais et al. 2011, 2013). In addition to dinoflagellates, the mixotrophic ciliate *Mesodinium rubrum* is an important primary producer, suggested to benefit from higher temperatures in the Gulf of Finland (GOF, Lips & Lips 2017) and Bothnian Sea (BS, Kuosa et al. 2017). Furthermore, precipitation is projected to increase by 30% in the northern Baltic, which would result in increased river discharge, and thus increase levels of allochthonous organic matter (e.g. humic substances) and organic pollutants (Andersson et al. 2015), causing a decrease in light availability for phototrophic growth. This is expected to have drastic effects on the Baltic Sea food web, such as enhanced growth of heterotrophic bacteria at the expense of phytoplankton (Sandberg et al. 2004), which might also open niches for non-native species (Andersson et al. 2015).

Diatoms sink to the seafloor rapidly after N is depleted in the photic zone (von Bodungen et al. 1981), and thus play a major role in C cycling by pelagic–benthic coupling (Heiskanen 1998).

Higher abundances of dinoflagellates may alter biogeochemical cycles, since higher C:P and C:N ratios in cultured dinoflagellates compared to diatoms have been reported (Quigg et al. 2003). However, the opposite (higher C:N and C:P) was found in diatom-dominated communities in mesocosm experiments with Baltic Sea spring communities (Spilling et al. 2014). During these experiments, the seston N:P ratio decreased with increasing dinoflagellate abundance after nutrient depletion, but no community effects were observed during exponential growth (Spilling et al. 2014). Some dinoflagellates (e.g. the toxic *Alexandrium tamarense*) require lower inorganic N:P ratios than other plankton (Shi et al. 2005) and can outcompete diatoms at low supply ratios (Hodgkiss & Ho 1997). A decrease in N:P supply ratios during the spring bloom is typical for the GOF (northern Baltic Sea), which is dominated by

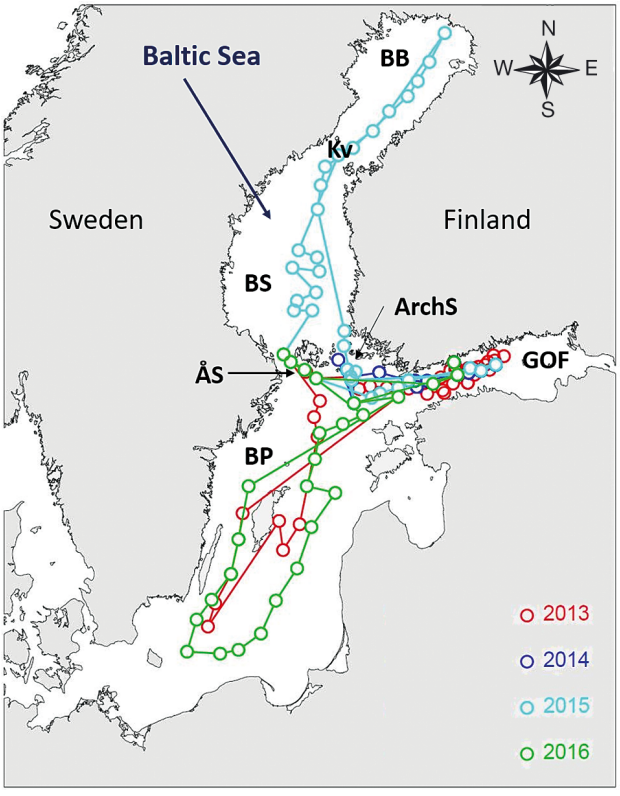

Fig. 1. Baltic Sea with sampled sub-basins in **bold**. The sailing routes of the research cruises (2013–2016) onboard the R/V 'Aranda' are depicted, and each dot represents a sampling station (n = 119). BB, BS: Bothnian Bay and Bothnian Sea, respectively; KV: Kvarken; ArchS: Archipelago Sea; Ås: Åland Sea; GOF: Gulf of Finland; BP: Baltic Proper

vertically migrating dinoflagellates and ciliates (*M. rubrum* and heterotrophic species) (Heiskanen 1995, Lips et al. 2014) and is N limited after the spring bloom (Tamminen & Andersen 2007).

The stoichiometric responses of monocultures may not be applicable to natural communities, with different species of autotrophs and heterotrophs in various life stages and diverse detrital particles (Frigstad et al. 2011). During the Baltic Sea spring bloom, the amount of detritus in the surface water was found to be constant and rather low, most likely due to high sinking rates common for this season (Heiskanen 1998, Lipsewers & Spilling 2018). Additionally, the stoichiometric range within the same species may be substantial, depending on environmental variables and interaction effects (Spilling et al. 2015). Thus, it is important to investigate potential environmental and community effects on stoichiometry in natural communities.

To understand the effects of changing phytoplankton spring bloom communities on seston stoichiometry in the Baltic Sea and improve our prediction of future shifts in its biogeochemistry, we investigated (1) the environmental drivers of the variability in nano- and microplankton community composition and (2) the effects of different communities and bloom phases on seston stoichiometry (C:N:P:Si:chl *a*). Based on the literature, we expected higher seston C:N, C:P, and chl *a*:C ratios during diatom dominance compared to dinoflagellate dominance; increasing C:N and C:P after the depletion of inorganic nutrients; and the lowest N:P ratios during the early phase of the spring bloom when phytoplankton growth is not limited by inorganic nutrients. Surface water samples were collected during 4 research cruises onboard the R/V 'Aranda', covering 7 sub-basins of the Baltic Sea and the whole course of the spring bloom combined.

2. MATERIALS AND METHODS

2.1. Cruises and sampling

The research cruises (2013–2016) differed in duration, sampled sub-basins, and bloom phases (Fig. 1). All samples (n = 119) were taken with a CTD rosette sampler from 3 m depth. A complete list of measured abiotic and biotic variables can be found in Tables 1 & 2.

2.2. Chl *a* and organic/inorganic nutrients

To determine chl *a* concentration as a proxy for phytoplankton biomass, 100 to 200 ml of seawater was filtered onto glass fiber filters (GF/F, 0.7 µm pore size, Whatman) in duplicates. Chl *a* was extracted in 10 ml of ethanol (96% v/v) and stored at −20°C until measurement (samples at room temperature [RT]) with a fluorescence spectrophotometer (Cary Eclipse, Varian Inc.) calibrated with chl *a* standards (Sigma Aldrich) (Jespersen & Christoffersen 1987).

To determine particulate organic carbon (POC), particulate organic nitrogen (PON), and particulate organic phosphorus (POP) concentrations, 100 to 200 ml samples were filtered using glass funnels onto acid-washed (HCl, 10% v/v) and pre-combusted (450°C, 4 h) GF/F filters. The filters were air dried and stored at RT until simultaneous analysis of POC and PON by mass spectrometry (Europa Scientific ANCA-MS 20-20) according to Koistinen et al.(2020a) and (2020b), respectively (see references therein). POP was determined by spectrophotometry using the protocol of Solórzano & Sharp (1980). Biogenic

silicate (BSi) samples (50–200 ml) were filtered using plastic funnels onto polycarbonate filters (0.8 µm mesh size, Poretics^{TM}, GVS), and dried filters were stored at RT until analysis. Before spectrophotometry, a wet alkaline digestion method was used to convert BSi to silicic acid (Krausse et al. 1983). Except for chl *a*:C (weight), seston ratios were calculated based on molar concentrations. In the following, we refer to POC:PON as the seston C:N ratio.

Dissolved inorganic nutrients (nitrate [NO_3^-], nitrite [NO_2^-], ammonium [NH_4^+], phosphate [PO_4^{3-}], and dissolved silicate [DSi]) were determined directly after sampling using spectrophotometry and standard colorimetric methods (Grasshoff et al. 2009).

2.3. Plankton community composition and estimation of C biomass

Plankton samples (200 ml) were preserved with acidic Lugol's solution (0.5% v/v) and stored in the dark at 4°C until microscopy. Samples (RT) were prepared according to Utermöhl (1958). Sub-samples of 10 to 50 ml were used for cell sedimentation (24–48 h) into counting chambers (HydroBIOS) after gentle mixing. Plankton cells were identified and enumerated by inverted microscopy (Leitz DM IRB, Leica). Details on the counting procedure and subsequent calculations (biovolume and C biomass) were recently published (Lipsewers & Spilling 2018 and references therein). Taxonomy was done with the aid of guides by Hällfors & Hällfors (2003) and Hällfors (2004), except for heterotrophic ciliates, which were identified based on Gruner (1981) and https://denstoredanske.lex.dk/ciliater (in Danish).

For data analysis, the microscopy-derived carbon (MDC) for 49 taxa (<100 µm size fraction) was considered. Rarely found taxa of diatoms and dinoflagellates were summarized to 'DIATOMS_other' and 'DINOS_other', small autotrophic and mixotrophic flagellates to 'FlagellateComplex', and heterotrophic nanoflagellates to 'HNFcomplex' (Table S1 in the Supplement at www.int-res.com/articles/suppl/m644p015_supp.pdf). The biomass of dominant heterotrophic ciliates (tintinnids, *Lohmaniella oviformis*, unidentified taxa) was pooled, and a group of dinoflagellates indistinguishable by traditional microscopy of Lugol's samples (*Gymnodinium corollarium*, *Biecheleria baltica*, and *Apocalathium malmogiense*) was termed 'DinoComplex', leaving 22 taxonomic units for further analyses.

The diatom–dinoflagellate proportion (DDP) was calculated: DDP = diatom biomass/(diatom biomass + dinoflagellate biomass). Wasmund et al. (2017) developed the DDP (based on wet weight) as a sub-basin specific index, whereas we used the MDC to calculate the DDP for each station (DDP >0.5 = diatom dominance, DDP <0.5 = dinoflagellate dominance).

2.4. Upper mixed layer depth (UMLD)

The UMLD was determined based on the stratification index *E* (Heiskanen & Kononen 1994, modified by Kuosa et al. 2017), calculated for additive water layers in 5 m steps: $E = [(\text{density}_{Deep} - \text{density}_{Surface}) \times 1000]/\text{bottom depth}$. Density_{Deep} is the density at 5 m depth for the first interval and 10 m for the second interval, until the maximum CTD depth of a station, and $\text{density}_{Surface}$ was measured at 1 m depth. A change of $E \geq 0.9$ (ΔE) between 2 water layers (e.g. 5–10 and 10–15 m) was defined as the UMLD (e.g. 12.5 m). When no ΔE was detected (linear depth profile), the water was considered fully mixed (bottom depth = UMLD). See Fig. S1 in the Supplement for 2 examples. Thermoclines above a water depth of 20 m are usually short term during the Baltic spring, but considering the more stable halocline instead (when UMLD <13 m) did not affect the outcome of the statistics; thus, only the shallower UMLDs were considered.

2.5. Bloom phases and primary production

Four different bloom phases (growth, peak, decline, and post-bloom) were defined based on concentrations of dissolved inorganic nutrients and chl *a*. Our data were compared to historical reports from individual sub-basins, and defined the growth phase as low chl *a*/high nutrient, peak as high chl *a*/low nutrient, decline as intermediate chl *a*/depleted nutrient, and post bloom as low chl *a*/depleted nutrient. More details on the concentration limits of the considered nutrients and chl *a* for individual sub-basins can be found in Spilling et al. (2019).

Primary production data are presented in Spilling et al. (2019); here, we used gross primary production (GPP). In short, seawater was collected, and radiolabeled bicarbonate solution (DHI) was added to a final specific activity of 0.1 µCi ^{14}C ml^{-1}. The samples were incubated in light (50 µmol photons m^{-2} s^{-1}, Philips TL 20 W fluorescent lamps) at ambient tem-

perature (climate chamber), and incubations were stopped with the addition of HCl (100 µl, 2 M) after 2 h. The open vials stayed in a fume hood (24 h) before adding 7 ml of scintillation cocktail (Instagel Plus, Perkin Elmer). The ^{14}C incorporation was determined with a liquid scintillation counter (Wallac Winspectral 1414). Dissolved inorganic carbon (DIC) was measured with a Unicarbo high-temperature combustion gas analyzer (Electro-Dynamo Oy), and GPP was calculated considering the total DIC pool and the fraction of radiolabeled ^{14}C fixed during the incubation period (Gargas 1975).

2.6. Statistical analyses

All linear and other regressions mentioned in Section 3, the corresponding curve fitting (r^2 and p-values), and preparation of box plots were done with SigmaPlot 10. The stoichiometric ratios and GPP were log transformed and analyzed with ANOVA on ranks (except for chl *a*:C, equal variance), as the groups had unequal variance (heteroscedasticity). Dunn's method (post hoc test) of pairwise multiple comparisons was applied to test the variability in seston stoichiometry and GPP between different bloom phases, whereas a Tukey's test (post hoc test) was used for chl *a*:C. This analysis was done with SigmaPlot 13 (Table 3, see Section 6 in the Supplement for details).

For all multivariate analyses, R (version 3.4.4, R Core Team 2014) and RStudio (1.1.442, RStudio Team 2015) were used. A redundancy analysis (RDA, maximum 200 permutations) using forward selection (R package vegan, Oksanen et al. 2013) was done to identify the environmental factors (explanatory variables, including chl *a* as one of the indicators for the bloom phases) affecting plankton community composition (response variables). Prior to the RDA, the MDC (µg C l^{-1}, n = 119) of the 22 groups and the UMLD were log transformed, and wind speed was raised to the power of 3 (Omstedt & Axell 2003). Fifteen environmental variables were analyzed (Table S3), and only the significant ones were considered for the final model (RDA plot). Highly correlated variables (variance inflation factors [VIFs] >10) were excluded before the final RDA. The analysis included an ANOVA-like permutation test (function anova.cca, for RDA under the reduced model, permutations: free, number of permutations: 999) to find the most parsimonious model. The collinearity (VIF values) of significant environmental variables ($p < 0.05$) was tested again before running the final model (see Fig. 3).

A community ordination (non-metric multidimensional scaling, NMDS) and generalized additive models (GAMs) were used to identify links between the dominant taxa and stoichiometric ratios of particulate organic nutrients, chl *a*:C, and GPP (response variables). BSi-related ratios and GPP were log transformed prior to the NMDS, whereas the taxon-specific MDC (plankton community matrix) was square root transformed followed by a Wisconsin standardization (see Fig. 5). The corresponding Shepard plot is shown in Fig. S2. To quantify the effect of community composition on, and the variability of, the response variables, the coordinates of each community (sampling station) along NMDS axes 1 and 2 were used as explanatory variables in separate GAMs, using R packages vegan (metaMDS function) and mgcv (Wood 2016). The response variables were used to color the symbols in the resulting NMDS plots (see Fig. 5), using R packages colorRamps (Keitt 2008) and plotrix (Lemon 2006).

3. RESULTS

3.1. Biotic and abiotic variables

There were substantial differences in biotic and abiotic variables between bloom phases and sub-basins (Tables 1 & 2). Temperature increased throughout the bloom, and average temperatures (±SD) at the growth, peak, decline, and post-bloom phases were 1.58 ± 0.57, 3.09 ± 1.28, 3.74 ± 1.51, and 4.85 ± 0.55°C, respectively. The most shallow UMLD detected was 7.5 m; thus, our surface samples (z = 3 m) represented this layer at all sampling stations.

High chl *a* and GPP were observed at low temperatures (Tables 1 & 2). The DDP ($r^2 = 0.30$) and chl *a* concentration ($r^2 = 0.31$) correlated negatively ($p < 0.0001$, linear regressions) with increasing temperature. The overall autotrophic contribution to biomass, measured as the chl *a*:C ratio, was lowest in the decline and post-bloom phases when the temperature was highest (Table 2). The highest biomass and GPP were found in the GOF, and the Bay of Bothnia featured clear differences, i.e. low temperature, salinity, chl *a*, and PO_4^{3-}, compared to the other sub-basins (Table 2).

3.2. Plankton community composition and important environmental drivers

Average autotrophic biomass (chl *a* ± SD) increased during the growth phase of the bloom (11.07

± 6.48 µg l^{-1}) before it gradually decreased from the peak phase (11.51 ± 4.31 µg l^{-1}) to the post-bloom phase (2.03 ± 0.74 µg l^{-1}, Fig. 2). The total MDC and POC (also µg l^{-1}) correlated positively with chl *a* (linear regressions, r^2 = 0.638 and 0.565, respectively, $p < 0.0001$). Five taxa within dinoflagellates, ciliates, and diatoms contributed >65% of the total MDC, with heterotrophic ciliates being the most important heterotrophs (Fig. 2, Table S2). After the bloom peak, community composition changed towards higher proportions of heterotrophic plankton (Fig. 2).

The community composition was mostly affected by temperature, DSi, UMLD ($p = 0.002$), $NO_2^- + NO_3^-$ ($p = 0.006$), PO_4^{3-} ($p = 0.022$), and NH_4^+ ($p = 0.038$) concentrations. Other explanatory variables of community composition (Section 7 in the Supplement) were location (latitude, longitude, bottom depth) and overall autotrophic biomass (chl *a*). Many diatoms (most notably *Thalassiosira baltica*, *T. levanderi*, *Chaetoceros* spp., *Achnanthes taeniata*) featured higher biomasses at lower temperatures and higher latitudes. The diatom *Melosira arctica* was overall less abundant and more important at high concentrations of dissolved inorganic N. The biomass of certain taxa (heterotrophic ciliates, Gymnodiniales, cyanobacteria) correlated positively with higher temperatures (lower latitudes) and PO_4^{3-} concentrations. A higher chl *a* concentration was found in shallow (coastal) waters at higher longitudes (mainly GOF), which is supported by the positive correlation between the UMLD and bottom depth (Fig. 3).

Community composition clearly varied between different bloom phases (Fig. 2, see Fig. 5). Most of the diatoms formed a cluster in the lower part of the NMDS plot (see

Table 1. Environmental variables (average ± SD) significantly affecting community composition and salinity divided by year and sub-basin. UMLD: upper mixed layer depth; nitrite (NO_2^-), nitrate (NO_3^-), ammonium (NH_4^+), phosphate (PO_4^{3-}), and silicate represent dissolved inorganic nutrients; Depth max.: bottom depth. Duration of the cruises (2013–2016), number of stations, and bloom phases sampled in each sub-basin are stated. Sub-basins: Gulf of Finland (GOF), Baltic Proper (BP), Åland Sea (ÅS), Archipelago Sea (ArchS), Bothnian Sea (BS), Kvarken (narrow strait, Kv), Bothnian Bay (BB). Bloom phases: Growth (Gr), Decline (Dec), post bloom (PB). **Bold**: characteristics for different seasons and sub-basins

Duration	Sub-basin	No. of stations	Bloom phase	Temperature (°C)	Salinity	UMLD (m)	Depth max. (m)	$NO_2^- + NO_3^-$ (µM)	NH_4^+ (µM)	PO_4^{3-} (µM)	Silicate (µM)
2013											
10–26	GOF	26	Gr, Peak, Dec	**1.43 ± 0.35**	5.56 ± 0.33	19.3 ± 7.5	61.0 ± 15.6	1.298 ± 1.768	0.168 ± 0.064	0.281 ± 0.078	12.44 ± 3.80
April	BP	10	Gr, Peak, Dec	**2.09 ± 0.32**	6.78 ± 0.45	48.0 ± 21.6	92.0 ± 46.1	0.760 ± 0.715	0.083 ± 0.038	0.243 ± 0.105	11.71 ± 2.23
	ÅS	3	Peak	**1.41 ± 0.17**	5.60 ± 0.20	15.8 ± 7.6	187.0 ± 12.1	0.030 ± 0.030	0.102 ± 0.024	0.040 ± 0.020	9.46 ± 0.75
2014											
5–10	GOF	9	Dec, PB	4.75 ± 0.30	5.64 ± 0.33	27.9 ± 12.0	58.3 ± 25.2	0.029 ± 0.087	0.109 ± 0.061	0.180 ± 0.075	7.62 ± 2.06
May	BP	1	PB	4.62	6.63	57.5	225.0	0.00	0.054	0.28	11.9
	ArchS	5	Dec, PB	4.77 ± 0.34	6.17 ± 0.17	60.7 ± 35.5	78.4 ± 34.2	0.152 ± 0.209	0.087 ± 0.016	0.286 ± 0.062	7.76 ± 1.12
2015											
4–15	GOF	5	Dec, PB	4.64 ± 0.55	5.34 ± 0.34	20.6 ± 11.7	66.8 ± 22.5	0.004 ± 0.009	0.179 ± 0.151	0.296 ± 0.08	9.22 ± 2.62
May	BP	4	Dec, PB	5.03 ± 0.49	6.05 ± 0.36	30.0 ± 22.5	101.3 ± 79.3	0.228 ± 0.207	0.171 ± 0.122	0.338 ± 0.056	10.43 ± 1.91
	ÅS	4	Dec	5.68 ± 0.51	5.62 ± 0.30	119.3 ± 127.5	211.3 ± 52.7	0.003 ± 0.005	0.025 ± 0.024	0.100 ± 0.080	7.65 ± 1.00
	ArchS	6	Peak, PB	5.10 ± 0.69	6.20 ± 0.29	64.4 ± 28.04	73.8 ± 28.1	0.060 ± 0.092	0.109 ± 0.027	0.222 ± 0.116	8.33 ± 2.14
	BS	10	Peak	3.83 ± 0.18	5.43 ± 0.16	76.7 ± 23.7	97.3 ± 27.3	0.065 ± 0.124	0.096 ± 0.028	0.120 ± 0.071	10.34 ± 1.39
	Kv	4	Peak, Dec	3.45 ± 1.09	3.90 ± 0.87	29.6 ± 20.0	49.8 ± 21.0	**2.498 ± 2.448**	**0.085 ± 0.028**	**0.005 ± 0.010**	24.08 ± 12.00
	BB	5	Dec	**1.92 ± 0.47**	**2.95 ± 0.42**	43.6 ± 26.8	57.4 ± 26.8	**5.558 ± 1.256**	**0.150 ± 0.114**	**0.006 ± 0.005**	38.56 ± 10.13
2016											
04–15	GOF	4	Gr, Peak, Dec	**2.23 ± 0.66**	5.03 ± 0.12	12.1 ± 7.1	59.0 ± 29.0	2.624 ± 3.125	0.161 ± 0.043	0.498 ± 0.134	15.97 ± 3.35
April	BP	19	Gr, Peak, Dec, PB	4.35 ± 0.78	7.03 ± 0.51	41.2 ± 20.6	123.4 ± 55.2	0.119 ± 0.430	0.106 ± 0.047	0.426 ± 0.108	15.11 ± 1.69
	ÅS	4	Peak	3.00 ± 0.20	5.56 ± 0.08	22.5 ± 8.2	214.0 ± 50.0	0.073 ± 0.073	0.135 ± 0.033	0.152 ± 0.033	17.16 ± 1.12

Table 2. Biological variables (average ± SD) considered for data analyses, divided by year and sub-basin. Gross primary production (GPP) and diatom–dinoflagellate proportion (DDP, modified after Wasmund et al. 2017) are based on microscopy-derived carbon. Stoichiometric ratios of particulate organic nutrients and chl *a* are given. Si: silicate (all seston). Order from top to bottom and abbreviations as in Table 1. **Bold**: characteristics for different seasons and sub-basins

Sub-basin	Chl *a* (µg l^{-1})	GPP (µmol C l^{-1} h^{-1})	DDP (µg C l^{-1})	Chl *a*:C (weight)	C:N (molar)	C:P (molar)	N:P (molar)	C:Si (molar)	N:Si (molar)
2013									
GOF	**14.7 ± 2.7**	**2.055 ± 0.840**	**0.58 ± 0.13**	**0.024 ± 0.003**	7.25 ± 0.54	105.86 ± 16.71	14.60 ± 2.24	10.60 ± 3.20	1.47 ± 0.46
BP	5.7 ± 1.5	0.728 ± 0.446	0.46 ± 0.29	**0.018 ± 0.005**	7.75 ± 0.50	116.16 ± 19.06	15.06 ± 2.68	20.69 ± 15.77	2.68 ± 2.04
ÅS	8.9 ± 3.3	1.450 ± 0.281	**0.57 ± 0.19**	**0.020 ± 0.003**	7.55 ± 0.33	87.01 ± 30.28	11.53 ± 4.00	5.84 ± 2.15	0.77 ± 0.28
2014									
GOF	6.1 ± 2.7	0.910 ± 0.652	**0.19 ± 0.09**	0.015 ± 0.003	7.22 ± 0.82	102.91 ± 22.47	14.16 ± 2.02	24.70 ± 16.34	3.44 ± 2.22
BP	**1.5**	0.372	**0.00**	0.006	8.27	109.20	13.20	23.54	2.85
ArchS	**1.4 ± 0.7**	0.380 ± 0.120	**0.28 ± 0.16**	0.008 ± 0.003	6.97 ± 0.51	91.78 ± 4.88	13.24 ± 1.44	11.16 ± 1.46	1.61 ± 0.27
2015									
GOF	7.8 ± 3.4	0.012 ± 0.004	0.20 ± 0.14	0.011 ± 0.002	8.82 ± 0.48	151.89 ± 16.22	17.22 ± 1.73	17.34 ± 7.43	1.97 ± 0.85
BP	4.1 ± 1.7	0.007 ± 0.005	0.18 ± 0.11	0.009 ± 0.002	9.02 ± 0.96	179.77 ± 41.33	19.77 ± 2.36	16.25 ± 1.12	1.81 ± 0.11
ÅS	3.6 ± 0.8	0.005 ± 0.001	0.46 ± 0.21	0.011 ± 0.002	8.97 ± 1.39	180.34 ± 31.52	20.64 ± 5.22	11.61 ± 4.63	1.35 ± 0.60
ArchS	4.7 ± 3.3	0.007 ± 0.004	0.15 ± 0.10	0.010 ± 0.005	8.47 ± 0.55	176.26 ± 30.81	20.76 ± 2.96	13.64 ± 4.15	1.61 ± 0.47
BS	10.6 ± 2.3	0.018 ± 0.008	**0.73 ± 0.14**	0.021 ± 0.006	9.05 ± 0.63	195.67 ± 28.04	21.74 ± 3.50	6.49 ± 3.61	0.73 ± 0.42
Kv	4.9 ± 1.9	0.003 ± 0.002	0.63 ± 0.04	0.014 ± 0.001	10.09 ± 0.98	210.33 ± 31.22	21.05 ± 3.92	9.12 ± 1.98	0.92 ± 0.26
BB	**2.3 ± 0.59**	0.001 ± 0.000	0.59 ± 0.17	0.011 ± 0.004	9.97 ± 0.96	191.47 ± 43.23	19.10 ± 3.26	10.91 ± 5.90	1.07 ± 0.48
2016									
GOF	**19.9 ± 7.4**	0.994 ± 0.651	0.35 ± 0.29	0.032 ± 0.010	6.96 ± 0.70	113.51 ± 10.06	16.49 ± 7.15	15.34 ± 7.05	2.26 ± 1.19
BP	5.9 ± 3.1	0.471 ± 0.219	0.08 ± 0.16	0.011 ± 0.004	7.49 ± 1.08	185.96 ± 63.13	24.44 ± 5.71	56.34 ± 36.66	7.58 ± 4.60
ÅS	9.2 ± 1.2	1.317 ± 0.38	**0.72 ± 0.09**	0.016 ± 0.001	9.90 ± 0.65	172.21 ± 19.65	17.43 ± 2.04	14.07 ± 3.47	1.42 ± 0.35

Fig. 5), linked to the growth phase of the bloom. Certain diatoms (e.g. *A. taeniata*) and DinoComplex were found at a high chl *a* concentration in the growth and peak phases of the bloom. The heterotrophic silicoflagellate *Ebria tripartita* (<2% MDC) was associated with the growing diatom population. Species succession was also observed within the diatom community: *T. levanderi*, *A. taeniata*, and *Chaetoceros* spp. peaked during the growth phase, *T. baltica* at the peak phase, and *Skeletonema marinoi* during the decline phase. Overall, however, the share of diatoms decreased, whereas heterotrophic organisms, most notably ciliates and heterotrophic nanoflagellates (HNF), and smaller plankton (FlagellateComplex) increased throughout the bloom. The share of dinoflagellates and *Mesodinium rubrum* was relatively constant, but some heterotrophic dinoflagellates (e.g. *Protoperidinium* spp., Gymnodiniales) became more abundant as the bloom progressed (Fig. 2).

3.3. Seston stoichiometry

Seston stoichiometry differed significantly between bloom-phases (Fig. 4), except for BSi-related ratios. Average C:N:P ratios were as follows: growth C_{103}:N_{14}:P_1, peak C_{144}:N_{18}:P_1, decline C_{136}:N_{17}:P_1, and post-bloom C_{127}:N_{17}:P_1 (total average C_{132}:N_{17}:P_1, n = 119). Compared to the growth phase of the bloom, variabilities in C:N, C:P, and N:P were higher during peak, decline, and post-bloom phases (size of boxes in Fig. 4).

Average C:N and C:P ratios were significantly lower and close to the Redfield ratio during the growth phase compared to the peak phase ($p \leq 0.005$), and C:P also differed between the growth and decline phases ($p = 0.005$) (Fig. 4, Table 3). During the post-bloom phase, average C:N and C:P ratios were closer to the values at the growth phase again (Fig. 4). The aver-

Table 3. ANOVA results for comparisons of 4 ratios at different bloom phases. The complete ANOVA report is shown in Section 5 in the Supplement (www.int-res.com/articles/suppl/m644p015_supp.pdf). **Bold**: $p < 0.05$

Ratio	Comparison	p	Ratio	p
Chl *a*:C	Growth vs. peak	0.635	C:N	**0.005**
	Growth vs. decline	**<0.001**		0.079
	Growth vs. post bloom	**<0.001**		1.000
	Peak vs. decline	**<0.001**		1.000
	Peak vs. post bloom	**<0.001**		0.183
	Decline vs. post bloom	**<0.002**		1.000
C:P	Growth vs. peak	**0.001**	N:P	**0.015**
	Growth vs. decline	**0.005**		**0.027**
	Growth vs. post bloom	1.000		1.000
	Peak vs. decline	1.000		1.000
	Peak vs. post bloom	0.164		0.500
	Decline vs. post bloom	0.362		0.749

age N:P was 14 during the growth phase and increased ($p \leq 0.027$) during the peak and decline phases of the bloom. However, during the post-bloom phase, it was close to 16 and not significantly different ($p \geq 0.5$) compared to the growth phase (Fig. 4D, Table 3). C:Si and N:Si ratios were not affected by the bloom phases and ranged from 17.7 to 18.9 and 2.4 to 2.9, respectively (Table 2). The chl *a*:C ratio decreased significantly ($p < 0.001$) from the peak to the post-bloom phase (Fig. 4A, Table 3, Section 6 in the Supplement), and variability decreased throughout the bloom phases (Fig. 4).

There were clear effects of plankton community composition on seston chl *a*:C, C:Si, and N:Si and weaker or no effects on the other ratios (Fig. 5, Fig. S3). All GAMs were significant ($p \leq 0.01$), and based on r^2 values (Fig. 5), the community composition explained ~45% of the variability in the chl *a*:C ratio, ~28% in N:P, ~20% in C:P, and ~8% in C:N. The latter was better explained by using the coordinates of each community along the *y*-axis of the NMDS plot (MDS 2, Fig. 5) explanatory variables ($r^2 = 0.244$, $p < 0.0001$), but it was virtually unaffected by the community composition.

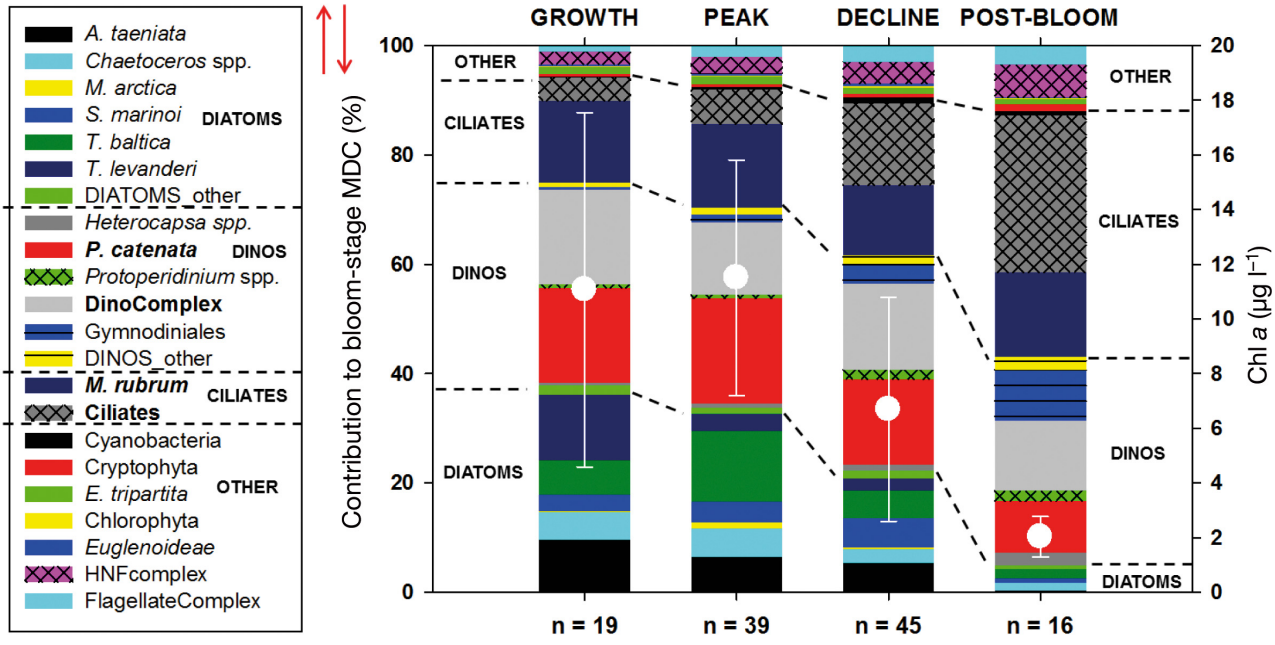

Fig. 2. Nano- and microplankton communities at different bloom phases. Stacked bars represent absolute contributions of 22 taxa to microscopy-derived carbon (MDC) in percent (left *y*-axis). Red arrows (top-right of the key) indicate that the order of taxa in the key is opposite the one in the stacked bars. The 4 most abundant taxa, considering the whole dataset, are in **bold** in the key (e.g. *Mesodinium rubrum*). Colors of stacks are repeating but not within 1 group (e.g. DIATOMS). Stacks with check patterns indicate heterotrophic taxa, line pattern indicates mixed groups, and remaining stacks represent autotrophic and mixotrophic groups. Bloom phases are shown on the top *x*-axis and the number of samples (n) on the bottom *x*-axis. Dashed lines represent trends of the 4 main groups (DIATOMS, DINOS [dinoflagellates], CILIATES, OTHER) along with the bloom. White circles represent average chl *a* concentration (right *y*-axis); error bars represent SD. *A. taeniata*: *Achnanthes taeniata*; *M. arctica*: *Melosira arctica*; *S. marinoi*: *Skeletonema marinoi*; *T. baltica*: *Thalassiosira baltica*; *T. levanderi*: *Thalassiosira levanderi*; DIATOMS_other: rarely found diatom taxa; *P. catenata*: *Peridiniella catenata*; DinoComplex: indistinguishable dinoflagellates; DINOS_other: rarely found dinoflagellate taxa; *M. rubrum*: *Mesodinium rubrum*; *E. tripartita*: *Ebria tripartita*; HNFcomplex: heterotrophic nanoflagellates; FlagellateComplex: small autotrophic and mixotrophic flagellates

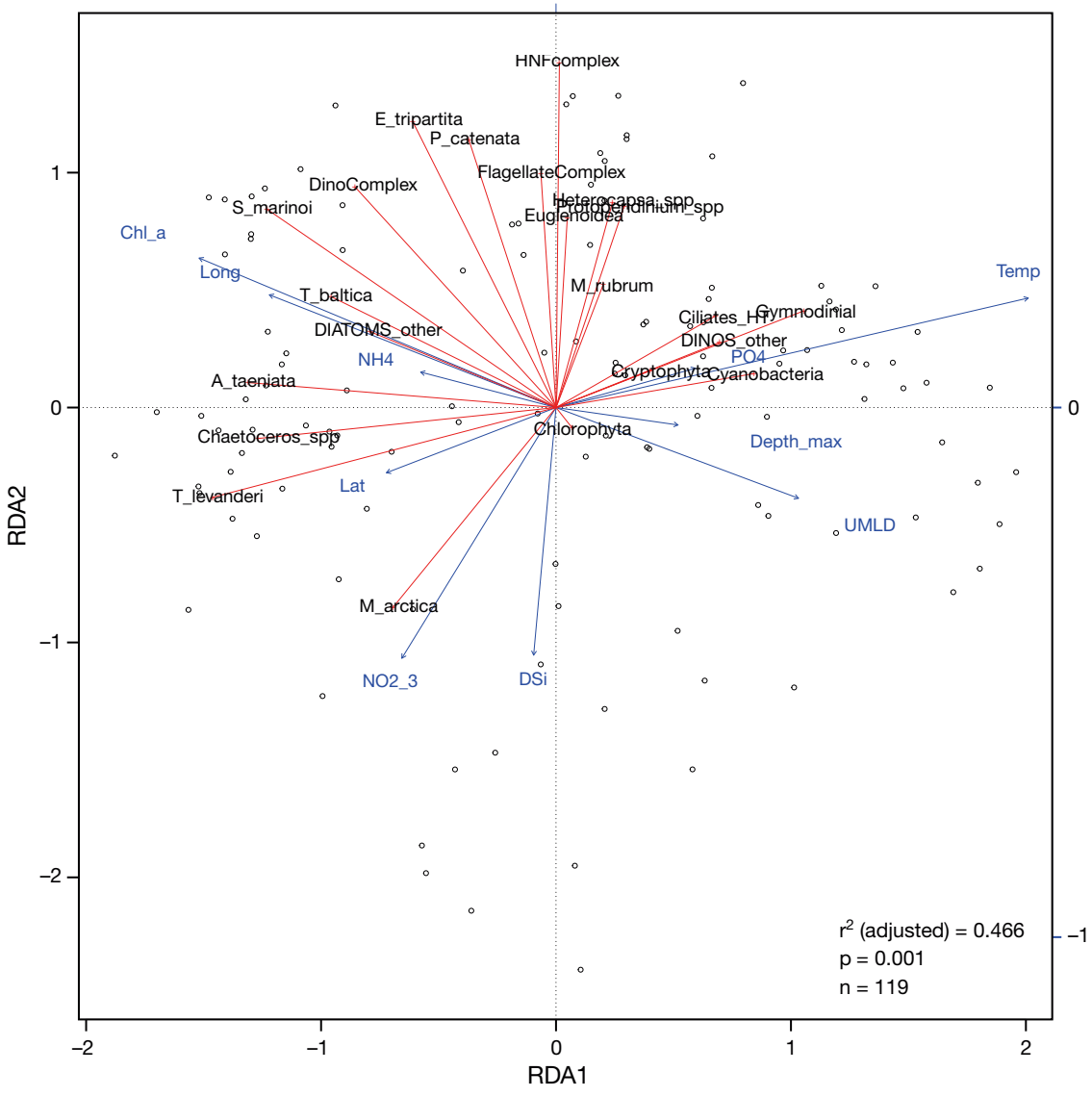

Fig. 3. Redundancy analysis (RDA) forward selection with environmental variables significantly affecting community composition. The adjusted r^2 value and p-value (ANOVA-like permutation test) represent the most parsimonious model considered for this RDA plot. Blue arrows represent explanatory variables, and r^2 values (longer arrow = higher r^2): temperature (Temp), dissolved silicate (DSi), latitude (Lat), chl_*a*, longitude (Long), depth of the upper mixed layer (UMLD), sum of nitrite and nitrate (NO2_3), bottom depth (depth_max, m), phosphate (PO4), and ammonium (NH4). Nutrients represent dissolved inorganic forms (µmol l^{-1}). Red arrows represent response variables: 22 taxa of nano-and microplankton organisms based on their C biomass (microscopy-derived carbon, n = 119). Ciliates_HT: heterotrophic ciliates; other abbreviations as in Fig. 2

At most stations, the C:N ratio was above the Redfield ratio of 6.6 (mostly 6–12). The stations with higher diversity and proportions of diatoms (growth phase) generally featured lower C:N ratios (6.2–7.6) compared to later bloom phases and dominance of *T. baltica* (8.9–11.5). The C:P ratio was clearly above the Redfield ratio of 106 at most stations and ranged from 65 to 334. The lower ratios (65–132) were found at high biomass and diversity of diatoms. The highest C:P ratios (>200) were found during late bloom phases with high abundances of *T. baltica*, certain dinoflagellates (e.g. Gymnodiniales and unidentified species), and cyanobacteria (Fig. S3). The N:P ratio ranged from 9 to 38 and increased with phytoplankton diversity, following the growth phase of the bloom, when the inorganic nutrient concentrations were low. The lowest N:P ratios (≤16) were found associated with diatom-dominated communities and low temperature (<3°C, Fig. S3). Slightly higher N:P ratios (>18) were found when *T. baltica* was more abundant and the highest ratios (>25) were associated with a higher diversity and water temperature (post-bloom, ≤5°C).

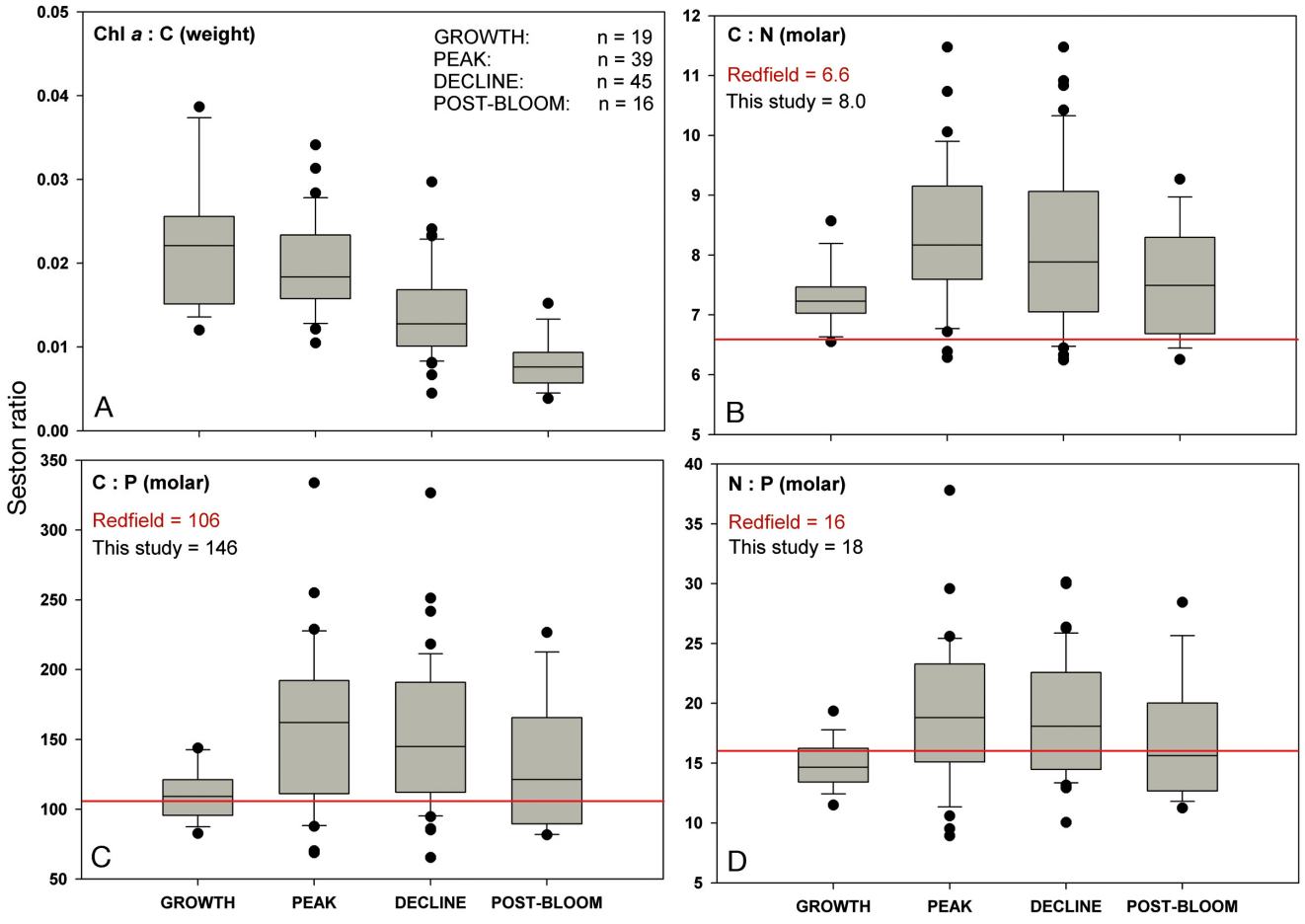

Fig. 4. Box plots of seston ratios significantly differing between bloom phases (horizontal line in boxes: median; box: 25–75 percentiles; whiskers: 10–90 percentiles; dots: outliers). Note different *y*-axis scales. Numbers of samples from different bloom phases (n) are given in (A). In (B–D), red lines indicate Redfield ratios (also stated in plots). Average ratios of this study (n = 119) are given as well. Corresponding ANOVA results are shown in Table 3

Seston C:Si and N:Si ratios were significantly ($p < 0.0001$) affected by the community composition (GAMs, $r^2 = 0.478$ and 0.473, respectively, Fig. 5, Fig. S3). These ratios were lowest at high proportions of diatoms and *E. tripartita*, and minimum values (C:Si = 1.3–2.0; N:Si = 0.3–0.9) were associated with *T. baltica* dominance (40–67 % of MDC). The highest ratios were found at high contributions of dinoflagellates (e.g. Gymnodiniales) and heterotrophic ciliates. Both BSi-related ratios decreased (exponential decay, $p < 0.0001$) with increasing *T. baltica* biomass ($r^2 = 0.39$ and 0.41, respectively). Diatom cell size (average biovolume cell^{-1} station^{-1}) correlated slightly ($r^2 = 0.116$, $p < 0.0001$) with the BSi concentration, indicating higher BSi contents in large species, such as *T. baltica* (≤110 µm cell diameter). The chl *a*:C ratio (~0.02–0.04) was positively correlated with diatom biomass (linear regression, $r^2 = 0.499$, $p < 0.0001$, Fig. 5), and was not correlated to any other taxonomic group to the same extent ($r^2 < 0.1$). This ratio was high (≥0.03) during the dominance of *T. baltica*. However, some dinoflagellates, such as DinoComplex and *Peridiniella catenata*, were abundant during maximum values of the chl *a*:C ratio (~0.04). GPP featured the same trend as chl *a*:C, and was higher at diatom-dominated stations during the growth phase of the bloom (GAM, $r^2 = 0.577$, $p < 0.0001$).

4. DISCUSSION

4.1. Plankton community composition and its driving forces

The community composition of nano- and microplankton differed between bloom phases, and the succession of taxa agrees with previous studies of the Baltic Sea spring bloom (Höglander et al. 2004, Le-

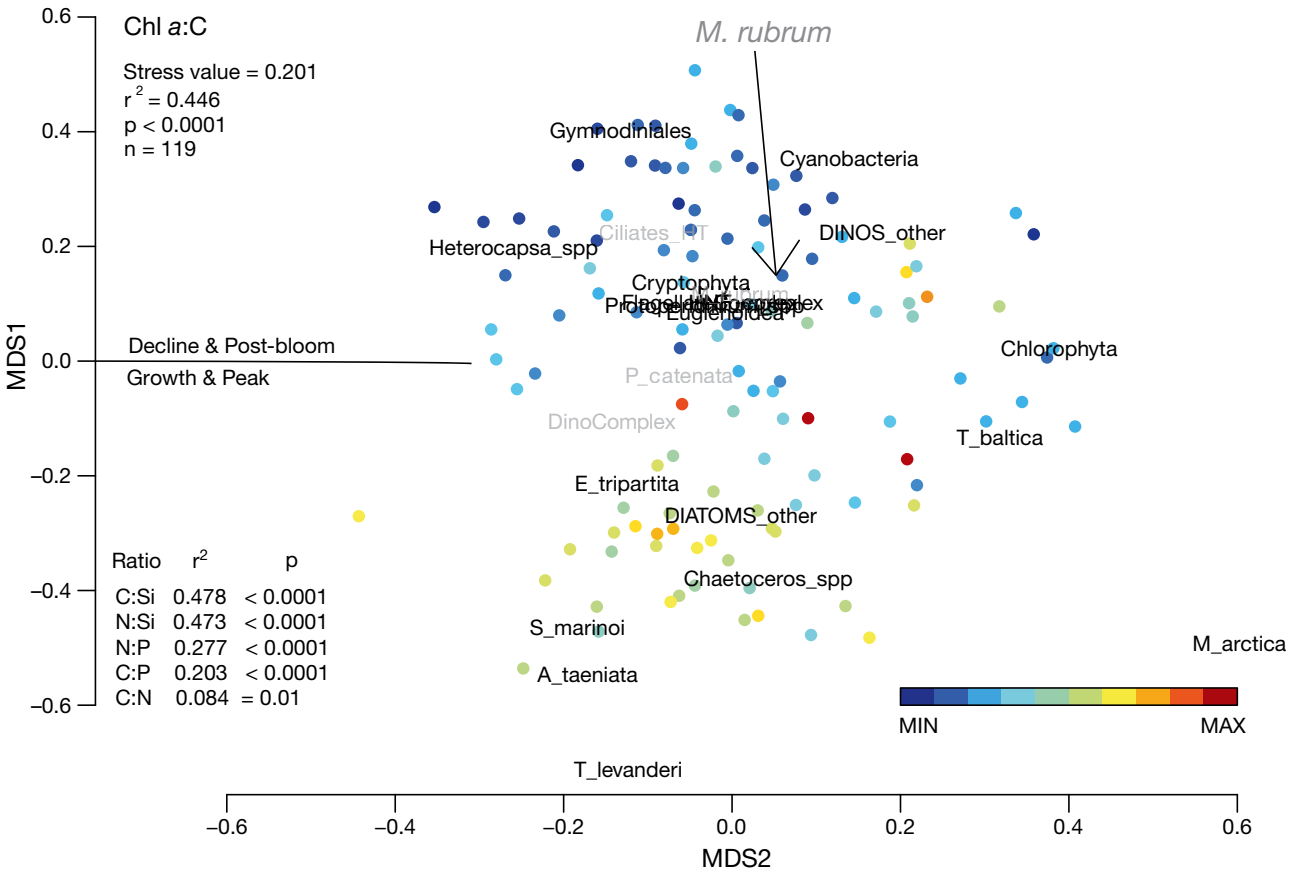

Fig. 5. Community ordination (non-metric multidimensional scaling) based on C biomass of 22 taxa. The effect of community composition on the chl *a*:C ratio is shown as an example. r^2 and p-values shown in the figure were obtained by generalized additive models, using the coordinates of each community along the multidimensional scaling (MDS) 1 axis as explanatory variables. Seston ratios were the response variables. Results for the other seston ratios are shown in the table in the lower left corner. See Fig. S3 in the Supplement (www.int-res.com/articles/suppl/m644p015_supp.pdf) for plots of C:N:P, C:Si, and N:Si ratios. Symbols are colored by the chl *a*:C ratio (MIN: minimum; MAX: maximum). The black horizontal line separates the bloom phases growth and peak from the decline and post-bloom phases based on community composition. The 4 most relevant taxa are represented by grey labels, and font size is equivalent to the relative biomass proportions (e.g. *Mesodinium rubrum* has the largest font size, see arrow indicating its position). Other taxa are shown in the same font size with black labels. Stress value (0.201), number of observations (n = 119), and arrangement of taxa were identical for all 6 seston ratios. Ciliates_HT: heterotrophic ciliates; other abbreviations as in Fig. 2

grand et al. 2015, Spilling et al. 2018). Diatoms produce higher biomass at lower temperatures (Finkel et al. 2010) and feature high growth rates at high inorganic nutrient concentrations and turbulent conditions (Margalef 1978, Smayda & Reynolds 2001). After inorganic N is depleted, they rapidly sediment out of the surface water (von Bodungen et al. 1981), quickly reducing the pelagic biomass concentration following the peak of the spring bloom (Reynolds & Wiseman 1982, Riebesell 1989). This is supported by the declining proportion of diatoms we observed at later bloom phases. The relative proportion of motile dinoflagellates was high and relatively constant (~40%) throughout the bloom. As expected, there was a development from autotrophic dominance (mainly diatoms and dinoflagellates) during the growth phase of the bloom towards a more heterotrophic community (high proportions of heterotrophic ciliates) after the depletion of inorganic nutrients.

Higher temperatures, reducing sea ice cover and promoting an earlier onset of stratification, are known to favor dinoflagellate growth before and during the bloom (Klais et al. 2013, Kremp 2013). We did not find a relationship between the UMLD and dinoflagellate proportion, but higher phytoplankton biomass was associated with a shallower UMLD. This was linked to coastal, which generally feature higher biological productivity than open, waters (Brink 2004).

The mixotrophic ciliate *Mesodinium rubrum* is an important primary producer in May and June in the GOF (Lips & Lips 2017) and was one of the most important species in our study. *M. rubrum* contributed a large proportion of the biomass at all bloom phases (~14–17%) as well as several subbasins (e.g. BS ≤28%). Our findings support recent studies suggesting that *M. rubrum* will benefit from increasing temperatures and become more abundant in the northern Baltic Sea (Kuosa et al. 2017). By vertical migration and efficient nutrient uptake, *M. rubrum* might outcompete phytoplankton for nutrients and may affect nutrient dynamics after the onset of stratification (Stoecker et al. 1991, Lips & Lips 2017). Generally, higher proportions of smaller taxa at later bloom phases are due to their larger surface to volume ratio (e.g. Lindemann et al. 2016), allowing more efficient nutrient uptake, and higher abundances of grazers usually coincide with increasing numbers of prey items such as bacteria (Alonso-Sáez et al. 2007, Camarena-Gómez et al. 2018). The heterotrophic silicoflagellate *Ebria tripartita* (low MDC) was associated with the growing diatom population and is known to feed on this phytoplankton group (Hargraves 2002). Thus, exponentially growing diatoms represent optimal conditions for this species, and decreasing diatom proportions will negatively affect its abundances. *E. tripartita* could be an important link to higher trophic levels during the spring bloom, similar to heterotrophic ciliates at later bloom phases and higher temperatures (Mironova et al. 2012, Lipsewers & Spilling 2018).

Increased temperatures leading to increased stratification and decreased nutrient availability in surface waters have been predicted for the Baltic Sea region (e.g. Meier et al. 2012, Thomas et al. 2017). In addition to dinoflagellates, these conditions are known to favor smaller taxa, i.e. picoplankton (Irwin & Oliver 2009), and their importance will likely increase in the future, highlighting the need to include these organisms in future studies on seston stoichiometry.

4.2. Effects of varying plankton communities on seston nutrient stoichiometry

Our average seston ratios, C:P 146, C:N 8, and N:P 18, were very similar to the average values for oceanic particulate matter, i.e. C:P 143, C:N 7.7, and N:P 19 (Sterner & Elser 2002). The variation of elemental ratios in marine systems is lower compared to freshwater habitats but generally more C rich (C_{166}:N_{20}:P_1) than the canonical Redfield ratio (Sterner et al. 2008). This agrees with our findings (C_{132}:N_{17}:P_1, average, n = 119) and suggests that the fixed C per inorganic nutrient unit is higher than 106:16:1 in the Baltic Sea as well, which is supported by a recent modeling study from the Gulf of Bothnia (Fransner et al. 2018). However, the seston C:N:P ratio varies regionally (Martiny et al. 2013), indicating that the average oceanic C:N:P ratio is plastic and might change over time, based on abiotic and biotic interactions (Garcia et al. 2018).

Considering all seston ratios, chl *a*:C was most significantly affected by the bloom phases, and community composition was responsible for 45% of the variation in this ratio. The chl *a*:C ratio (also GPP) was generally higher in diatom-dominated communities, which could be due to their rapid synthesis of chl *a* (Ross & Geider 2009). Diatoms are also known to have a generally higher chl *a* content than dinoflagellates (Finkel et al. 2010), and this agrees with findings from enclosure experiments with Baltic Sea spring communities (Spilling et al. 2014). Interestingly, the presented ratio varied within a fixed range (~0.005–0.04), irrespective of the taxon considered for the correlation. Also, some clearly dinoflagellate-dominated communities featured high chl *a*:C ratios (0.04), suggesting that it is more difficult to draw clear conclusions regarding community composition at high ratios, indicating autotrophic dominance over heterotrophs (e.g. Vargas et al. 2007). However, the probability for diatom-dominated chl *a*:C ratios increases with increasing ratios. The availability of light, nutrients, and temperature are well known to influence pigment concentration in phytoplankton cells (Chan 1980, Neale et al. 1989). This causes the large variation of chl *a*:C ratios observed in nature, which do not always seem to be taxonomically affected (Jakobsen & Markager 2016).

Like the chl *a*:C ratio, C:Si and N:Si ratios were most obviously explained by community structure (~47%) and, not surprisingly, by diatom biomass. These ratios did not differ between bloom phases, suggesting that the diatom community comprised stable C:Si and N:Si contents, although its biomass decreased drastically after the peak of the bloom. Kremp et al. (2008) reported that diatom resting stages, formed at the end of the spring bloom, feature high silicate concentrations; thus, one could expect differences in BSi-related ratios between peak and post-bloom phases, but this was not detected in our data. Growth-limiting concentrations of DSi for diatoms typically occur at <2 µmol DSi l^{-1} (Egge & Aksnes 1992) and were not detected in the present study. Diatoms could also be outcompeted by non-

silicifying organisms (e.g. flagellates, Officer & Ryther 1980) at increased molar supply ratios of N:DSi >2 (Gilpin et al. 2004). The Baltic Sea diatoms are currently not DSi limited during the spring bloom (Wasmund et al. 2013), but it could limit the production of highly silicified resting spores at the end of the growth season (Kremp et al. 2008), potentially affecting the biomass of vegetative cells in the following growing season.

Community composition explained 28% of the variability in N:P, 20% in C:P, and only 8% in C:N. Spilling et al. (2014) found a stronger community effect on the C:N ratio, but they reported almost complete dominance (>90% biomass) of either diatoms or dinoflagellates, whereas they contributed equal shares (~40% MDC) at growth and peak phases in our study. Field studies and experimental studies are difficult to compare, as the export of organic matter is an important factor in natural waters and not considered in many enclosure experiments.

4.3. Temporal development of seston nutrient stoichiometry

There was a temporal development in the C:N:P ratio, which was significantly higher ($p \leq 0.015$) at the peak compared to the growth phase, despite highly similar community compositions. This indicates that other factors also contributed to the presented stoichiometry, which was likely affected by the different bloom phases to a larger extent than merely species composition. These factors include physiological processes such as primary production and C storage (Sterner & Elser 2002), which might have increased the C:N:P ratio towards the peak phase (Fig. 4). At the bloom peak, inorganic nutrients reach limiting concentrations, while the plankton community continues to assimilate C (e.g. Banse 1994), resulting in increasing C:N ratios due to the uncoupling of C and N dynamics common for phytoplankton blooms (e.g. Wetz & Wheeler 2003, Taucher et al. 2012). This C overconsumption (Toggweiler 1993) is common at later bloom phases and related to higher temperatures (Taucher et al. 2012) and nutrient stress (Biddanda & Benner 1997, Wetz & Wheeler 2003), which are also known to elevate C:P and N:P ratios (Martiny et al. 2016). Additionally, a higher cell content of P-rich ribosomes is needed at high growth rates (Goldman et al. 1979), and more ribosomes per cell are required for the same protein synthesis when temperature decreases (Toseland et al. 2013). Even though Toseland et al. (2013) considered a much greater temperature range, including the tropics, this could be the mechanism explaining lower N:P and C:P ratios during the growth phase since our range spans winter and spring conditions in the Baltic Sea. The average C:N:P ratio of 132:17:1 we found in the Baltic Sea was close to the ratio found in warm, nutrient-rich upwelling regions (137:18:1, Martiny et al. 2013), and the lowest C:N:P ratio of 103:14:1 (<2°C, growth phase, our data) was also observed in cold, nutrient-rich water by others (78:13:1, Martiny et al. 2013).

After the peak, the C:N:P ratio decreased towards the decline and post-bloom phases. This coincided with decreasing plankton biomass and increasing proportions of microzooplankton (heterotrophic ciliates), nanozooplankton (mostly HNFcomplex), and smaller phytoplankton (<10 µm, e.g. FlagellateComplex, Fig. 2, details in Spilling et al. 2019). Their active growth (e.g. higher ribosome content) using (recycled) nutrients at least contributed to the decreasing C:N:P ratios. Additionally, dinoflagellates are known to have high uptake affinities for P and continue its assimilation even after they stop growing (Kremp et al. 2008). There is typically a surplus of PO_4^{3-} at the end of the spring bloom (also in presented data) in most of the Baltic Sea basins (especially in the GOF), and luxury uptake could have decreased C:P and N:P ratios. In addition, zooplankton and heterotrophic bacteria typically have higher cell-specific P contents compared to autotrophs (Andersen & Hessen 1991, Vadstein 2000, Sterner & Elser 2002), and their increasing share of the seston (especially microzooplankton) in combination with the reasons above likely caused the reduction in C:N:P after the bloom peak (Frigstad et al. 2011). Considering the definition of Sieburth et al. (1978), picoplankton (e.g. heterotrophic bacteria) pass the pores of GF/F filters (0.7 µm) at least to some extent. However, the Baltic spring bloom is dominated by large-celled and chain-forming taxa, limiting the C flux through picoplankton (Lignell et al. 1993). Mesozooplankton was excluded from our results due to the applied microscopy method. Thus, the exact contribution of these organisms to the presented seston stoichiometry is unknown.

The C:N:P ratios at the growth and post-bloom phases were very similar, despite notable differences in community composition, biomass, and temperature. Thus, the taxonomic composition could only explain the variability in seston stoichiometry to a relatively low extent. Identifying all drivers of the variability in seston stoichiometry was not part of this study and is not trivial. This is partially because field

samples include a tremendous variability in cell activity, community structure, and origin of different particles (Frigstad et al. 2011). According to Frigstad et al. (2011), detritus can contribute a significant proportion of the total seston. Even though the concentration of detrital particles was estimated to be constant and rather low in the presented data (Lipsewers & Spilling 2018), it would be interesting to identify and quantify all seston compartments and study their effect on stoichiometry in different bloom phases. Additionally, the organic particles collected on a filter represent a snapshot of the highly dynamic natural processes affecting seston stoichiometry. The P content of a cell is highly variable; thus, C:N is more stable than C:P during seasonal changes (Martiny et al. 2016). This is independent of species composition, and community activity supersedes taxonomic effects in this case. Environmental variables (temperature, light, inorganic nutrients) determine plankton community physiology, structure, and biomass. Both abiotic and biotic factors, individually and by interaction effects, cause variations in seston stoichiometry.

5. SUMMARY AND CONCLUSIONS

Overall, the nano- and microplankton community was dominated by autotrophic dinoflagellates (*Peridiniella catenata* and DinoComplex) and ciliates (*Mesodinium rubrum* and heterotrophs). The diatoms decreased along with the overall autotrophic contribution, GPP, and total biomass from the growth to the post-bloom phase. This succession was strongly linked to increasing temperature and decreasing inorganic nutrient concentrations. There was an overall development of increasing C:N:P ratios, from the growth to the peak phase of the bloom, followed by a reduction towards the decline and post-bloom phases. Plankton community composition affected seston ratios to different extents: it explained ~50% of the variability in C:Si, N:Si, and ch *a*:C and <30% of shifts in C:P and N:P, whereas C:N was virtually unaffected (8%). In terms of the predictability of variations in seston stoichiometry during the Baltic spring bloom, we found an upper limit for the chl *a*:C ratio of 0.04, unaffected by community composition, which might be useful as a maximum value for modeling studies. Diatoms determined the ranges of C:Si, N:Si (especially *Thalassiosira baltica*), and chl *a*:C. Thus, based on community composition, these ratios can be predicted with higher certainty than the Redfield-related ones (C:N:P).

We expected the highest seston C:N, C:P, and chl *a*:C ratios during diatom dominance and the lowest N:P ratios during the early phase of the bloom. Regarding chl *a*:C and N:P, our results matched these expectations based on the available literature. Regarding the Redfield-related ratios (C:N:P), we found higher values in more diverse communities with higher relative proportions of dinoflagellates and heterotrophic organisms compared to diatoms. However, the variations in C:N:P ratios were explained by community composition to only <30%. Thus, our findings from different bloom phases with different communities (e.g. growth vs. post bloom) suggest that the variation in these ratios is primarily driven by the collective community activity (physiology) rather than its structure, especially in natural mixed communities, which rarely feature absolute dominance of a single species.

Acknowledgements. We thank Dr. Harri Kuosa (SYKE) for the great support in manuscript preparation and determination of the UMLD, Johanna Oja (SYKE) for her help with microscopy, the water chemistry team (SYKE) for measuring inorganic nutrients, the staff of Tvärminne Zoological Station (University of Helsinki) for measuring particulate nutrients, the primary production team from the University of Vigo (Dr. C. Sobrino, D. Perez-Quemaliños, Dr. A. Fuentes), the R/V 'Aranda' and its crew for great technical support and catering, Alícia Martinez (University of Barcelona) for the help with sampling in 2016, and Juho Lappalainen (SYKE) for calculating the distances between stations and the shoreline. We used the SYKE marine research infrastructure (FINMARI). Funding was granted by the Academy of Finland (decision numbers 259164 and 263862), Onni Talas Foundation (T.L.), and Walter and Andrée de Nottbeck Foundation (M.T.C.G., K.S.).

LITERATURE CITED

Alonso-Sáez L, Arístegui J, Pinhassi J, Gómez-Consarnau L and others (2007) Bacterial assemblage structure and carbon metabolism along a productivity gradient in the NE Atlantic Ocean. Aquat Microb Ecol 46:43–53

Andersen T, Hessen DO (1991) Carbon, nitrogen, and phosphorus content of freshwater zooplankton. Limnol Oceanogr 36:807–814

Andersson A, Meier HM, Ripszam M, Rowe O and others (2015) Projected future climate change and Baltic Sea ecosystem management. Ambio 44:345–356

Arrigo KR (2005) Marine microorganisms and global nutrient cycles. Nature 437:349–355

Banse K (1994) Uptake of inorganic carbon and nitrate by marine plankton and the Redfield ratio. Global Biogeochem Cycles 8:81–84

Biddanda B, Benner R (1997) Carbon, nitrogen, and carbohydrate fluxes during the production of particulate and dissolved organic matter by marine phytoplankton. Limnol Oceanogr 42:506–518

Boyd PW, Lennartz ST, Glover DM, Doney SC (2015) Biological ramifications of climate-change-mediated ocea-

nic multi-stressors. Nat Clim Chang 5:71–79
Brink KH (2004) The grass is greener in the coastal ocean. https://www.whoi.edu/oceanus/feature/the-grass-is-greener-in-the-coastal-ocean/ (accessed 8 Nov 2019)
Camarena-Gómez MT, Lipsewers T, Piiparinen J, Eronen-Rasimus E and others (2018) Shifts in phytoplankton community structure modify bacterial production, abundance and community composition. Aquat Microb Ecol 81:149–170
Chan AT (1980) Comparative physiological study of marine diatoms and dinoflagellates in relation to irradiance and cell size. II. Relationship between photosynthesis, growth, and carbon/chlorophyll *a* ratio. J Phycol 16: 428–432
Ducklow HW, Steinberg DK, Buesseler KO (2001) Upper ocean carbon export and the biological pump. J Oceanogr 14:50–58
Egge JK, Aksnes DL (1992) Silicate as regulating nutrient in phytoplankton competition. Mar Ecol Prog Ser 83: 281–289
Falkowski PG, Raven JA (1997) Carbon acquisition and assimilation. In: Falkowski PG, Raven JA (eds) Aquatic photosynthesis. Blackwell Science, Oxford, p 128–162
Field CB, Behrenfeld MJ, Randerson JT, Falkowski P (1998) Primary production of the biosphere: integrating terrestrial and oceanic components. Science 281:237–240
Finkel ZV, Quigg A, Raven J, Reinfelder J, Schofield O, Falkowski P (2006) Irradiance and the elemental stoichiometry of marine phytoplankton. Limnol Oceanogr 51:2690–2701
Finkel ZV, Beardall J, Flynn KJ, Quigg A, Rees TAV, Raven JA (2010) Phytoplankton in a changing world: cell size and elemental stoichiometry. J Plankton Res 32:119–137
Fleming RH (1940) The composition of plankton and units for reporting populations and production. Proc 6th Pac Sci Congr 3:535–540
Fransner F, Gustafsson E, Tedesco L, Vichi M and others (2018) Non-Redfieldian dynamics explain seasonal pCO_2 drawdown in the Gulf of Bothnia. J Geophys Res Oceans 123:166–188
Frigstad H, Andersen T, Hessen DO, Naustvoll LJ, Johnsen TM, Bellerby R (2011) Seasonal variation in marine C:N:P stoichiometry: Can the composition of seston explain stable Redfield ratios? Biogeosciences 8:2917–2933
Garcia NS, Sexton J, Riggins T, Brown J, Lomas MW, Martiny AC (2018) High variability in cellular stoichiometry of carbon, nitrogen, and phosphorus within classes of marine eukaryotic phytoplankton under sufficient nutrient conditions. Front Microbiol 9:543
Gargas E (1975) A manual for phytoplankton primary production studies in the Baltic. Vandkvalitetsinstituttet ATV, Hoersholm
Gilpin L, Davidson K, Roberts E (2004) The influence of changes in nitrogen:silicon ratios on diatom growth dynamics. J Sea Res 51:21–35
Goldman JC, McCarthy JJ, Peavey DG (1979) Growth rate influence on the chemical composition of phytoplankton in oceanic waters. Nature 279:210–215
Grasshoff K, Kremling K, Ehrhardt M (eds) (2009) Methods of seawater analysis. Wiley-VCH, Weinheim
Groetsch PM, Simis SG, Eleveld MA, Peters SW (2016) Spring blooms in the Baltic Sea have weakened but lengthened from 2000 to 2014. Biogeosciences 13: 4959–4973
Gruner HE (1981) Urania Tierreich: Wirbellose Tiere. In: Gruner HE (ed) Urania Tierreich Wirbellose Tiere 3. Urania Verlag, Berlin
Hällfors G (2004) Checklist of Baltic Sea phytoplankton species (including some heterotrophic protistan groups). Balt Sea Environ Proc 95, HELCOM, Helsinki
Hällfors S, Hällfors H (2003) Phytoplankton of the northern Baltic Sea — a guide for identification. Course material, University of Helsinki
Hargraves PE (2002) The ebridian flagellates *Ebria* and *Hermesinum*. Plankton Biol Ecol 49:9–16
Harris GP (1999) Comparison of the biogeochemistry of lakes and estuaries: ecosystem processes, functional groups, hysteresis effects and interactions between macro- and microbiology. Mar Freshw Res 50:791–811
Hecky R, Kilham P (1988) Nutrient limitation of phytoplankton in freshwater and marine environments: a review of recent evidence on the effects of enrichment 1. Limnol Oceanogr 33:796–822
Heiskanen AS (1995) Contamination of sediment trap fluxes by vertically migrating phototrophic micro-organisms in the coastal Baltic Sea. Mar Ecol Prog Ser 122:45–58
Heiskanen AS (1998) Factors governing sedimentation and pelagic nutrient cycles in the northern Baltic Sea. PhD dissertation, Finnish Environment Institute, Helsinki
Heiskanen AS, Kononen K (1994) Sedimentation of vernal and late summer phytoplankton communities in the coastal Baltic Sea. Arch Hydrobiol 131:175–198
HELCOM (2018) State of the Baltic Sea. http://stateofthebalticsea.helcom.fi (accessed 8 Nov 2019)
Hodgkiss IJ, Ho KC (1997) Are changes in N:P ratios in coastal waters the key to increased red tide blooms? Asia-Pacific Conference on Science and Management of Coastal Environment. Springer, p 141–147
Höglander H, Larsson U, Hajdu S (2004) Vertical distribution and settling of spring phytoplankton in the offshore NW Baltic Sea proper. Mar Ecol Prog Ser 283:15–27
Irwin AJ, Oliver MJ (2009) Are ocean deserts getting larger? Geophys Res Lett 36:L18609
Jakobsen HH, Markager S (2016) Carbon-to-chlorophyll ratio for phytoplankton in temperate coastal waters: seasonal patterns and relationship to nutrients. Limnol Oceanogr 61:1853–1868
Jespersen AAM, Christoffersen K (1987) Measurements of chlorophyll *a* from phytoplankton using ethanol as extraction solvent. Arch Hydrobiol 109:445–454
Keitt TH (2008) Coherent ecological dynamics induced by large-scale disturbance. Nature 454:331–334
Klais R, Tamminen T, Kremp A, Spilling K, Olli K (2011) Decadal-scale changes of dinoflagellates and diatoms in the anomalous Baltic Sea spring bloom. PLOS ONE 6:e21567
Klais R, Tamminen T, Kremp A, Spilling K, An BW, Hajdu S, Olli K (2013) Spring phytoplankton communities shaped by interannual weather variability and dispersal limitation: mechanisms of climate change effects on key coastal primary producers. Limnol Oceanogr 58:753–762
Klausmeier CA, Litchman E, Levin SA (2004) Phytoplankton growth and stoichiometry under multiple nutrient limitation. Limnol Oceanogr 49:1463–1470
Klausmeier CA, Litchman E, Daufresne T, Levin SA (2008) Phytoplankton stoichiometry. Ecol Res 23:479–485
Koistinen J, Sjöblom M, Spilling K (2020a) Determining inorganic and organic carbon. In: Spilling K (ed) Biofuels from algae: methods and protocols. Methods in molecular biology, Vol 1980. Humana Press, New York, NY, p 63–70

Koistinen J, Sjöblom M, Spilling K (2020b) Determining inorganic and organic nitrogen. In Spilling K (ed) Biofuels from algae: methods and protocols. Methods in molecular biology, Vol 1980. Humana Press, New York, NY, p 71–80

Krausse GL, Schelske CL, Davis CO (1983) Comparison of three wet-alkaline methods of digestion of biogenic silica in water. Freshw Biol 13:73–81

Kremp A (2013) Diversity of dinoflagellate life cycles: facets and implications of complex strategies. In: Lewis JM, Marret F, Bradley LR (eds) Biological and geological perspectives of dinoflagellates. The Micropalaeontological Society, Special Publications, Geological Society, London, p 189–198

Kremp A, Tamminen T, Spilling K (2008) Dinoflagellate bloom formation in natural assemblages with diatoms: nutrient competition and growth strategies in Baltic spring phytoplankton. Aquat Microb Ecol 50:181–196

Kuosa H, Fleming-Lehtinen V, Lehtinen S, Lehtiniemi M and others (2017) A retrospective view of the development of the Gulf of Bothnia ecosystem. J Mar Syst 167:78–92

Legrand C, Fridolfsson E, Bertos-Fortis M, Lindehoff E, Larsson P, Pinhassi J, Andersson A (2015) Interannual variability of phyto-bacterioplankton biomass and production in coastal and offshore waters of the Baltic Sea. Ambio 44:427–438

Lemon J (2006) Plotrix: a package in the red light district of R. R News 6:8–12

Lignell R, Heiskanen AS, Kuosa H, Gundersen K, Kuuppo-Leinikki P, Pajuniemi R, Uitto A (1993) Fate of a phytoplankton spring bloom: sedimentation and carbon flow in the planktonic food web in the northern Baltic. Mar Ecol Prog Ser 94:239–252

Lindemann C, Fiksen Ø, Andersen KH, Aksnes DL (2016) Scaling laws in phytoplankton nutrient uptake affinity. Front Mar Sci 3:26

Lips I, Lips U (2017) The importance of *Mesodinium rubrum* at post-spring bloom nutrient and phytoplankton dynamics in the vertically stratified Baltic Sea. Front Mar Sci 4:407

Lips I, Rünk N, Kikas V, Meerits A, Lips U (2014) High-resolution dynamics of the spring bloom in the Gulf of Finland of the Baltic Sea. J Mar Syst 129:135–149

Lipsewers T, Spilling K (2018) Microzooplankton, the missing link in Finnish plankton monitoring programs. Boreal Environ Res 23:127–137

Margalef R (1978) Life-forms of phytoplankton as survival alternatives in an unstable environment. Oceanol Acta 1: 493–509

Martiny AC, Pham CT, Primeau FW, Vrugt JA, Moore JK, Levin SA, Lomas MW (2013) Strong latitudinal patterns in the elemental ratios of marine plankton and organic matter. Nat Geosci 6:279–283

Martiny AC, Talarmin A, Mouginot C, Lee JA, Huang JS, Gellene AG, Caron DA (2016) Biogeochemical interactions control a temporal succession in the elemental composition of marine communities. Limnol Oceanogr 61:531–542

Meier HM, Andersson HC, Arheimer B, Blenckner T and others (2012) Comparing reconstructed past variations and future projections of the Baltic Sea ecosystem — first results from multi-model ensemble simulations. Environ Res Lett 7:034005

Mironova E, Telesh I, Skarlato S (2012) Diversity and seasonality in structure of ciliate communities in the Neva Estuary (Baltic Sea). J Plankton Res 34:208–220

Moreno AR, Martiny AC (2018) Ecological stoichiometry of ocean plankton. Annu Rev Mar Sci 10:43–69

Neale PJ, Cullen JJ, Yentsch CM (1989) Bio-optical inferences from chlorophyll *a* fluorescence: What kind of fluorescence is measured in flow cytometry? Limnol Oceanogr 34:1739–1748

Niemi Å (1973) Ecology of phytoplankton in the Tvärminne area, SW coast of Finland. I. Dynamics of hydrography, nutrients, chlorophyll *a* and phytoplankton. PhD dissertation, University of Helsinki

Officer CB, Ryther JH (1980) The possible importance of silicon in marine eutrophication. Mar Ecol Prog Ser 3:83–91

Okolodkov Y (1999) An ice-bound planktonic dinoflagellate *Peridiniella catenata* (Levander) Balech: morphology, ecology and distribution. Bot Mar 42:333–341

Oksanen J, Blanchet FG, Kindt R, Legendre P, Minchin PG, O'hara RB, Wagner H and others (2013) Community ecology package. R package version 2, https://cran.r-project.org, https://github.com/vegandevs/vegan

Omstedt A, Axell L (2003) Modeling the variations of salinity and temperature in the large gulfs of the Baltic Sea. Cont Shelf Res 23:265–294

Quigg A, Finkel ZV, Irwin AJ, Rosenthal Y and others (2003) The evolutionary inheritance of elemental stoichiometry in marine phytoplankton. Nature 425:291–294

R Core Team (2014) R: a language and environment for statistical computing. R Foundation for Statistical Computing, Vienna

Redfield AC (1934) On the proportions of organic derivatives in sea water and their relation to the composition of plankton. In: Daniel RJ (ed) James Johnstone Memorial Volume. University Press of Liverpool, p 176–192

Redfield AC (1958) The biological control of chemical factors in the environment. Am Sci 46: 205–221

Reynolds C, Wiseman S (1982) Sinking losses of phytoplankton in closed limnetic systems. J Plankton Res 4:489–522

Riebesell U (1989) Comparison of sinking and sedimentation rate measurements in a diatom winter/spring bloom. Mar Ecol Prog Ser 54:109–119

Ross ON, Geider RJ (2009) New cell-based model of photosynthesis and photo-acclimation: accumulation and mobilisation of energy reserves in phytoplankton. Mar Ecol Prog Ser 383:53–71

RStudio Team (2015) RStudio: integrated development for R. RStudio, Boston, MA

Sandberg J, Andersson A, Johansson S, Wikner J (2004) Pelagic food web structure and carbon budget in the northern Baltic Sea: potential importance of terrigenous carbon. Mar Ecol Prog Ser 268:13–29

Shi Y, Hu H, Cong W (2005) Positive effects of continuous low nitrate levels on growth and photosynthesis of *Alexandrium tamarense* (Gonyaulacales, Dinophyceae). Phycol Res 53:43–48

Sieburth JM, Smetacek V, Lenz J (1978) Pelagic ecosystem structure: heterotrophic compartments of the plankton and their relationship to plankton size fractions. 1. Limnol Oceanogr 23:1256–1263

Smayda TJ, Reynolds CS (2001) Community assembly in marine phytoplankton: application of recent models to harmful dinoflagellate blooms. J Plankton Res 23:447–461

Solórzano L, Sharp JH (1980) Determination of total dissolved phosphorus and particulate phosphorus in natural waters. 1. Limnol Oceanogr 25:754–758

Spilling K, Kremp A, Klais R, Olli K, Tamminen T (2014) Spring bloom community change modifies carbon path-

ways and C:N:P:chl *a* stoichiometry of coastal material fluxes. Biogeosciences 11:7275–7289

Spilling K, Ylöstalo P, Simis S, Seppälä J (2015) Interaction effects of light, temperature and nutrient limitations (N, P and Si) on growth, stoichiometry and photosynthetic parameters of the cold-water diatom *Chaetoceros wighamii*. PLOS ONE 10:e0126308

Spilling K, Olli K, Lehtoranta J, Kremp A and others (2018) Shifting diatom–dinoflagellate dominance during spring bloom in the Baltic Sea and its potential effects on biogeochemical cycling. Front Mar Sci 5:327

Spilling K, Fuentes-Lema A, Quemaliños D, Klais R, Sobrino C (2019) Primary production, carbon release, and respiration during spring bloom in the Baltic Sea. Limnol Oceanogr 64:1779–1789

Sterner RW, Elser JJ (2002) Ecological stoichiometry: the biology of elements from molecules to the biosphere. Princeton University Press, Princeton, NJ

Sterner RW, Andersen T, Elser JJ, Hessen DO, Hood JM, McCauley E, Urabe J (2008) Scale-dependent carbon: nitrogen:phosphorus seston stoichiometry in marine and freshwaters. Limnol Oceanogr 53:1169–1180

Stoecker DK, Putt M, Davis LH, Michaels AE (1991) Photosynthesis in *Mesodinium rubrum*: species-specific measurements and comparison to community rates. Mar Ecol Prog Ser 73:245–252

Talarmin A, Lomas MW, Bozec Y, Savoye N, Frigstad H, Karl DM, Martiny AC (2016) Seasonal and long-term changes in elemental concentrations and ratios of marine particulate organic matter. Global Biogeochem Cycles 30:1699–1711

Tamminen T, Andersen T (2007) Seasonal phytoplankton nutrient limitation patterns as revealed by bioassays over Baltic Sea gradients of salinity and eutrophication. Mar Ecol Prog Ser 340:121–138

Taucher J, Schulz KG, Dittmar T, Sommer U, Oschlies A, Riebesell U (2012) Enhanced carbon overconsumption in response to increasing temperatures during a mesocosm experiment. Biogeosciences 9:3531–3545

Thomas DN, Kaartokallio H, Tedesco L, Majaneva M and others (2017) Life associated with Baltic Sea ice. In: Snoeijs-Leijonmalm P, Schubert H, Radziejewska T (eds) Biological oceanography of the Baltic Sea. Springer, Dordrecht, p 333–357

Toggweiler JR (1993) Carbon overconsumption. Nature 363: 210–211

Toseland A, Daines SJ, Clark JR, Kirkham A and others (2013) The impact of temperature on marine phytoplankton resource allocation and metabolism. Nat Clim Chang 3:979

Tyrrell T (1999) The relative influences of nitrogen and phosphorus on oceanic primary production. Nature 400:525

Utermöhl H (1958) Zur Vervollkommnung der quantitativen Phytoplankton-Methodik. Mitt Int Ver Theor Angew Limnol 9:1–38

Vadstein O (2000) Heterotrophic, planktonic bacteria and cycling of phosphorus. In: Schink B (ed) Advances in microbial ecology. Springer, Boston, MA, p 115–167

Vargas CA, Martínez RA, Cuevas LA, Pavez MA and others (2007) The relative importance of microbial and classical food webs in a highly productive coastal upwelling area. Limnol Oceanogr 52:1495–1510

von Bodungen B, von Brockel K, Smetacek V, Zeitzschel B (1981) Growth and sedimentation of the phytoplankton spring bloom in the Bornholm Sea (Baltic Sea). Kieler Meeresforsch Sonderh 5:49–60

Wasmund N, Uhlig S (2003) Phytoplankton trends in the Baltic Sea. ICES J Mar Sci 60:177–186

Wasmund N, Nausch G, Feistel R (2013) Silicate consumption: an indicator for long-term trends in spring diatom development in the Baltic Sea. J Plankton Res 35:393–406

Wasmund N, Kownacka J, Göbel J, Jaanus A and others (2017) The diatom/dinoflagellate index as an indicator of ecosystem changes in the Baltic Sea. 1. Principle and handling instruction. Front Mar Sci 4:22

Wasmund N, Nausch G, Gerth M, Busch S, Burmeister C, Hansen R, Sadkowiak B (2019) Extension of the growing season of phytoplankton in the western Baltic Sea in response to climate change. Mar Ecol Prog Ser 622: 1–16

Wetz MS, Wheeler P (2003) Production and partitioning of organic matter during simulated phytoplankton blooms. Limnol Oceanogr 48:1808–1817

Wood S (2016) mgcv: GAMs with GCV/AIC/REML smoothness estimation and GAMMs by PQL. R package version 1.8-16

Editorial responsibility: Antonio Bode, A Coruña, Spain

Submitted: December 10, 2019; Accepted: May 7, 2020
Proofs received from author(s): June 15, 2020